Yersiniabactin is a quorum sensing autoinducer and siderophore in uropathogenic *Escherichia coli*

James R. Heffernan[a,b], George L. Katumba [a,b], William H. McCoy[c], Jeffrey P. Henderson[a,b]#

[a]Center for Women's Infectious Disease Research, Washington University School of Medicine, St. Louis, Missouri 63110, United States.

[b]Division of Infectious Diseases, Department of Internal Medicine, Washington University School of Medicine, St. Louis, Missouri 63110, United States.

[c]Division of Dermatology, Department of Internal Medicine, Washington University School of Medicine, St. Louis, Missouri 63110, United States.

Running title: Quorum sensing siderophore in uropathogenic *E. coli*

Address correspondence to Jeffrey P. Henderson, hendersonj@wustl.edu

Abstract word count: 175

Text word count: 3188

ABSTRACT

Siderophores are secreted ferric ion chelators used to obtain iron in nutrient-limited environmental niches, including human hosts. While all *E. coli* encode the enterobactin (Ent) siderophore system, isolates from patients with urinary tract infections additionally encode the genetically distinct yersiniabactin (Ybt) siderophore system. To determine whether the Ent and Ybt systems are functionally redundant for iron uptake, we compared growth of different isogenic siderophore biosynthesis mutants in the presence of transferrin, a human iron-binding protein. We observed that the Ybt system does not compensate for loss of the Ent system during siderophore-dependent, low density growth. Using transcriptional and product analysis, we found that this non-redundancy is attributable to a density-dependent transcriptional stimulation cycle in which Ybt assume an additional autoinducer function. These results distinguish the Ybt system as a combined quorum-sensing and siderophore system. These functions may reflect Ybt as a public good within bacterial communities or as an adaptation to confined, subcellular compartments in infected hosts. The efficiency of this arrangement may contribute to the extraintestinal pathogenic potential of *E. coli* and related *Enterobacterales.*

IMPORTANCE

Urinary tract infections (UTIs) are one of the most common human bacterial infections encountered by physicians. Adaptations that increase the pathogenic potential of commensal microbes such as *E.coli* are of great interest. One potential adaptation observed in clinical isolates is accumulation of multiple siderophore systems, which scavenge iron for nutritional use. While iron uptake is important for bacterial growth, the increased metabolic costs of siderophore production could diminish bacterial fitness during infections. In a siderophore-dependent growth conditions, we show that the virulence-associated yersiniabactin siderophore system in uropathogenic *E. coli* is not redundant with the ubiquitous *E. coli* enterobactin system. This arises not from differences in iron scavenging activity but because yersiniabactin is preferentially expressed during bacterial crowding, leaving bacteria dependent upon enterobactin for growth at low cell density. Notably, this regulatory mode arises because yersiniabactin

stimulates its own expression, acting as an autoinducer in a previously unappreciated quorum-sensing system. This unexpected result connects quorum-sensing with pathogenic potential in *E. coli* and related *Enterobacterales.*

30 **INTRODUCTION**

31 Urinary tract infections (UTIs) are one of the most common bacterial infections in clinics and
32 hospitals, with over 7 million doctor visits and 1 million emergency room visits in the United States each
33 year[1]. *Escherichia coli* account for ~85% of these infections and are a leading cause of recurrent UTIs[2,3].
34 As clinical *E. coli* isolates become increasingly resistant to first-line antibiotics, there is renewed interest
35 in better understanding features of these and related *Enterobacterales* that increase their pathogenic
36 potential in human hosts[4].

37 Among the most prominent host-pathogen interactions in UTIs is the interplay between human
38 factors that limit nutrient iron availability and the corresponding bacterial responses to iron scarcity[5,6].
39 Normal physiological iron excretion in humans is low, with most iron in the host bound to heme[7,8]. In
40 circulation and tissue, labile iron ions are sequestered by binding to transferrin, a circulating iron transport
41 protein that binds ferric ions in two iron binding pockets with K_a values of $4.7*10^{20}$ M^{-1} and $2.4*10^{19}$ M^{-1}
42 [9]. After the arrival of infecting bacteria, local innate immune responses in tissue intensify this iron
43 sequestration response by introducing additional iron-binding proteins. Epithelial cells and neutrophils
44 introduce lipocalin-2/siderocalin, which sequesters iron in complexes with catechol metabolites[10–12].
45 Lactoferrin, a member of the transferrin family excreted by neutrophils, can bind iron 300 times more
46 tightly than transferrin[13] and, like lipocalin-2, becomes detectible in the urine of patients with UTIs[14].
47 After bacteria establish an early infection, these innate immune responses intensify the baseline iron
48 restriction state maintained by transferrin.

49 Upon entering the host, infecting *E. coli* counteract host-mediated iron ion sequestration by
50 secreting specialized iron chelators called siderophores, which have been detected in urine from UTI
51 patients[11,15]. Siderophores are small molecules with affinities for iron (III) that make them competitive
52 with mammalian iron-binding proteins[16]. Iron (III)-siderophore complexes are avidly imported by
53 dedicated bacterial import systems to support nutritional demands for this critical, growth-limiting
54 nutrient. Intracellular iron released from siderophore complexes then participates in feedback repression
55 of siderophore biosynthetic genes through the ferric uptake regulator (Fur)[17,18]. The stereotypical, 19 base

56 sequence motif (the Fur box) involved in this regulatory arrangement is a common criterion for
57 identifying siderophore operons in genomic data[19].

58 *E. coli,* as well as many other *Enterobacterales* species, secrete the catechol-based siderophore
59 enterobactin (Ent), a siderophore with extraordinarily high iron (III) affinity ($K_a \sim 10^{52}$)[20]. Nevertheless, *E.*
60 *coli* isolates from patients with UTI encode up to three additional, genetically non-conserved siderophore
61 systems that import siderophores yersiniabactin (Ybt), salmochelin, and aerobactin, respectively. Ybt is
62 the non-Ent siderophore most frequently encountered in clinical urinary isolates[10,21–23], where it is
63 associated with increased pathogenic potential[4,24,25]. Why *E. coli* strains with elevated pathogenic
64 potential incur the additional metabolic cost of synthesizing additional siderophores is a longstanding
65 question. One rationale is that these non-conserved siderophores more effectively evade innate immune
66 responses than the Ent system. Another rationale, independent of iron acquisition, is that non-conserved
67 siderophore systems may benefit infection-associated *E. coli* strains through interactions with non-iron
68 transition metal ions, including copper[23] and nickel[22]. Given that a single siderophore may perform
69 multiple functions, these rationales are not mutually exclusive.

70 In the present study, we ask whether Ybt is functionally redundant with Ent for iron uptake. In
71 these experiments we compared growth of model uropathogenic *E. coli* (UPEC) strain UTI89 mutants
72 expressing only Ent or Ybt in the presence of human transferrin. We also chemically complemented
73 cultures of siderophore-deficient strains with purified Ent or Ybt. We used transcriptional reporter
74 constructs for siderophore biosynthetic genes to identify a non-canonical mode of regulation consistent
75 characteristic of quorum sensing systems. The results are consistent with a multifunctional role for Ybt
76 that includes autoinduction in a quorum-sensing regulation in addition to transition metal ion binding.

77 **RESULTS**

78 ***Siderophore-dependent UPEC growth in human transferrin-containing medium***

79 To determine whether the iron acquisition functions of UPEC siderophore systems are functionally
80 redundant, we first sought to establish a culture condition in which growth is dependent upon siderophore
81 production. The model UPEC strain UTI89 can secrete catecholate siderophores (enterobactin and
82 salmochelin) and a phenolate siderophore yersiniabactin (Ybt)[24]. Enterobactin produced by UTI89 may be
83 secreted directly or modified by C-glycosidation machinery encoded by the *iroA* cassette to form
84 salmochelin and other modified enterobactins. To identify a siderophore-dependent growth condition we
85 compared growth of UTI89 with its isogenic, siderophore-deficient mutant UTI89*ΔentBΔybtS*[24]. In
86 M63/nicotinic acid/0.2% glycerol medium, which has been previously demonstrated to stimulate UPEC
87 siderophore production[22,23,26], UTI89*ΔentBΔybtS* exhibited only a mild growth defect in late stationary
88 phase relative to UTI89 (see **Fig. S1a** in the supplemental material). In contrast, human transferrin (hTf)
89 addition, previously used to create a siderophore-dependent growth condition[27], led to a marked, highly
90 significant UTI89*ΔentBΔybtS* growth defect relative to UTI89 ($p<0.0001$ at 10 hours) (**Fig. S1b**). This
91 growth defect was not observed when hTf was replaced with heat-denatured hTf or an equivalent molar
92 amount of bovine serum albumin (**Fig. S1c, d**), consistent with a determinative role for intact hTf iron-
93 binding domains. $FeCl_3$ supplementation (10 μM) also abolished the hTf-associated UTI89*ΔentBΔybtS*
94 growth defect, consistent with an iron-dependent phenotype (**Fig. S1e**). Finally, substitution of hTf with
95 150 μM of the iron(III) chelator compound, 2,2'-dipyridyl replicated the UTI89*ΔentBΔybtS*[24] growth
96 defect observed with hTf ($p< 0.05$ at 10 hours)(**Fig. S1f**), which is also consistent with an iron-dependent
97 phenotype. Together, these data are consistent with M63/nicotinic acid/0.2% glycerol/hTf (hereafter
98 abbreviated as M63+hTf) as a siderophore-dependent growth condition.

99

100 ***Siderophore system contributions to siderophore-dependent growth***

101 To determine whether the Ent and Ybt systems are similarly capable of supporting siderophore-dependent
102 growth, we compared growth between UTI89 mutants expressing Ent or Ybt as the sole siderophore

103 (UTI89*ΔiroAΔybtS* and UTI89*ΔentB*, respectively) (**Table 1**). In the absence of hTf, both mutants grew
104 similarly to UTI89 (**Fig. 1a**). In the presence of hTf, UTI89*ΔiroAΔybtS* grew similarly to UTI89, but
105 UTI89*ΔentB* exhibited a profound growth deficiency comparable to the siderophore-deficient strain
106 UTI89*ΔentBΔybtS* ($p<0.0001$ at 10 hours) (**Fig. 1b**). Comparable results were obtained with substitution
107 of 2,2'-dipyridyl for hTf (**Fig. S2**). Together, these results are inconsistent with the hypothesis that the
108 Ybt siderophore system is functionally redundant with Ent system-mediated iron acquisition. The results
109 are consistent with a role for Ent, but not Ybt, in supporting UTI89 growth from low cellular density in
110 the presence of hTf.
111
112 ***Chemical complementation effects on siderophore-dependent growth***
113 We considered that non-redundancy of the Ybt system may arise from deficient Ybt siderophore activity
114 relative to Ent. To test this hypothesis, we chemically complemented UTI89*ΔentBΔybtS* in M63+hTf with
115 equimolar quantities of either purified Ent or Ybt. We observed a comparable dose-response relationship
116 for the two siderophores, reaching a maximal response at 3 μM for each (**Fig. 1c,d**). This result is
117 consistent with Ybt and Ent having equivalent siderophore activity in M63+hTf. Thus, the growth defect
118 of UTI89*ΔentB* in M63+hTf (**Fig. 1b**) is not due to an inability of Ybt to substitute for Ent's siderophore
119 activity.
120
121 ***Extracellular siderophore accumulation during siderophore-dependent growth***
122 We next considered the possibility that Ent and Ybt production differ in our siderophore-dependent
123 culture conditions. To compare siderophore production in M63+hTf, we used liquid chromatography-
124 mass spectrometry to quantify siderophores in conditioned media over time. In UTI89 cultures, Ybt
125 concentrations exhibited a delayed increase compared to Ent, paralleled the growth (optical density)
126 curve, and were maximal during stationary phase (**Fig. 2a**). In the Ent-deficient mutant UTI89*ΔentB*, Ybt
127 production kinetics were markedly depressed (**Fig. 2b**). Conversely, Ent production kinetics were
128 substantially unchanged in the Ybt-deficient mutant UTI89*ΔybtSΔiroA* (**Fig. 2c**). In the absence of hTf,

129 Ybt production kinetics by UTI89*ΔentB* and Ent production kinetics by UTI89*ΔybtSΔiroA* were both
130 comparable to UTI89 (**Fig. S3a,b,c**). These results are consistent with Ybt production during low
131 bacterial cell density culture that is insufficient to overcome the absence of Ent during siderophore-
132 dependent growth.
133
134 ***Ybt biosynthetic gene transcription is delayed during siderophore-dependent growth***
135 The disparate growth kinetics displayed by UTI89 siderophore mutants may reflect differences in
136 siderophore biosynthetic gene expression during early culture. To test early biosynthesis gene expression,
137 we used qRT-PCR to compare mRNA transcripts from early Ent and Ybt biosynthesis genes (*entB* and
138 *ybtS*, respectively) (**Table S1**). To accommodate the large media volumes necessary to obtain adequate
139 RNA yield from low density cultures, we substituted hTf with 2,2'-dipyridyl. At one hour of culture, the
140 expression fold change of *entB* was significantly higher than that of *ybtS* ($p=0.03$). By four hours, this
141 difference was diminished and became insignificant ($p>0.05$) (**Fig. 3**). This finding is consistent with a
142 UTI89 siderophore system transcriptional response that emphasizes Ent biosynthesis during early growth
143 and Ybt biosynthesis later in culture when cell density is greater.
144
145 ***Ybt biosynthetic gene upregulation delay is typical of culture populations***
146 To determine whether Ybt expression was delayed uniformly by cells in culture or is attributable to
147 distinct subpopulations, we created reporter plasmids in which Ent or Ybt biosynthetic operon promoters
148 drive expression of different fluorescent reporters and measured their activity with flow cytometry (**Fig.**
149 **S4a,b**) (**Table S1**). In *p:entC-mCherry*, the *entCEBA* promoter for the main Ent biosynthetic operon
150 controls mCherry expression. In *p:ybtP-GFP* the *Yersinia* HPI operon 1 promoter controlling
151 transcription of the first Ybt biosynthetic gene (*ybtS*) controls GFP expression[28](**Fig. 4a-d**). In M63+hTf,
152 mean fluorescence intensity (scaled to maximum value) of the *Yersinia* operon 1 reporter in UTI89
153 *p:entC-mCherry p:ybtP-GFP* was significantly delayed over the first 8 hours compared to the *entCEBA*

154 reporter (2 hours p=0.054, 4-8 hours p<0.05, 10 hours p=0.076) (**Fig. 4e)**. These results are consistent
155 with the qRT-PCR results and demonstrate a population-wide delay in Ybt biosynthetic gene upregulation
156 by UTI89 in M63+hTf. Differences in transcriptional activation may relate to inability of the Ybt system
157 to compensate for the loss of Ent during siderophore-dependent growth.
158
159 ***Fur repression does not account for delayed ybt production and expression***
160 We next examined how transcriptional control of Ent and Ybt biosynthesis differs. Fur (ferric uptake
161 regulator) is the canonical siderophore system regulator and participates in homeostatic feedback
162 repression by iron, though more complex regulatory schemes are possible[29–31]. To determine whether
163 more profound Fur repression explains delayed Ybt system transcription, we compared reporter
164 expression and siderophore production between UTI89 and its Fur-deficient mutant UTI89*Δfur*. We
165 observed that the late *Yersinia* operon 1 reporter stimulation observed in UTI89 persists in UTI89*Δfur*
166 when compared to *entCEBA* reporter (4-10 hours p<0.05) (**Fig. 4e,f**). There remains a corresponding,
167 significant delay in Ybt production relatively to Ent (4-10 hours p<0.05) (**Fig. 4g**). The retained delay in
168 Ybt biosynthetic upregulation is inconsistent with differential Fur regulation as the basis for kinetic
169 differences in Ent and Ybt biosynthesis in these conditions.
170
171 ***Ybt biosynthetic gene upregulation by Ent-null mutant is abolished during siderophore-dependent***
172 ***growth***
173 To determine whether transcriptional Ybt biosynthetic upregulation occurs in the UTI89*ΔentB*
174 background, we monitored reporter activity in UTI89*ΔentB p:entC-mCherry p:ybtP-GFP* during growth
175 in M63+hTf. In this strain, the increase in *Yersinia* operon 1 reporter MFI observed with the wild type
176 reporter strain was abolished for the duration of the assay (p<0.05, 10-20 hrs) (**Fig. 5a**). This is notable as
177 there is no known direct regulatory connection between the two siderophore systems and Ent-null UTI89
178 can grow and produce Ybt comparably to wild type UTI89 in the absence of competitive iron chelators
179 (**Fig S3**) [24]. We considered an indirect connection between the two siderophore systems in the M63+hTf

180 condition. We noted that differences in Ybt biosynthetic transcriptional activity between the wild type and
181 Ent-deficient reporter strains coincide with differences in culture density (5 hours p=.02, 6 hours p=.002,
182 7-20 hours p<0.001)(**Fig. 5b**). Ent stimulation in the Ent deficient mutant still expressed *entCEBA*
183 reporter at similar level during growth (0-15 hours p>0.05) **(Fig. S5)**. This suggested to us the possibility
184 of a density-dependent regulatory input on Ybt biosynthesis.
185
186 ***Ybt is an autoinducer***
187 We hypothesized that an important Ybt biosynthetic stimulus derives from the density-dependent
188 regulation characteristic of a quorum sensing (QS) system. A defining feature of QS systems is
189 production of a secreted molecule that accumulates outside the cell in proportion to population density.
190 This secreted molecule – an autoinducer - then upregulates its own production in a concentration-
191 dependent manner, creating a feed-forward autoregulatory loop. Although multiple QS systems have been
192 described in *E. coli*[32–35], we hypothesized that Ybt fulfills the autoinducer role in addition to its
193 siderophore role. To test this, we compared *Yersinia* operon 1 reporter activity between UTI89 *p:entC-*
194 *mCherry p:ybtP-GFP* and the Ybt biosynthesis-null mutant UTI89*ΔybtE p:entC-mCherry p:ybtP-GFP*
195 during siderophore-dependent growth in M63+hTf. Despite similar growth curves, the GFP reporter was
196 markedly suppressed in UTI89*ΔybtE* (**Fig. 5a).** At 20 hours MFI of *Yersinia* operon 1 reporter was
197 significantly diminished compared to UTI89 WT **(Fig. 6a,d)**. Chemical complementation of UTI89*ΔybtE*
198 *p:entC-mCherry p:ybtP-GFP* with purified Ybt restored GFP fluorescence (**Fig. 6b,d**), while equimolar
199 Ent did not (**Fig. 6c,d**). Together, these results distinguish Ybt production as subject to autoinductive
200 regulation in which Ybt plays a dual role as effector and signaling molecule. In this context, deficient Ybt
201 accumulation in the medium leads to inadequate Ybt autoinduction at low population density. Ent
202 production, in contrast, is activated independently of population density, facilitates entry into logarithmic
203 growth in M63+hTf, and facilitates higher Ybt production by the larger bacterial population.
204

205 ***YbtA is a candidate Ybt sensor***

206 Most QS systems follow a general functional model for density-dependent regulation[36–39]. Applying this
207 paradigm to the Ybt system, we anticipated a Ybt-specific response element that increases Ybt
208 biosynthesis. A prominent candidate for this receptor is the AraC-type transcription factor YbtA, which is
209 predicted to possess a ligand binding domain that may act as a Ybt sensor[28,40,41]. To assess the role of
210 YbtA in controlling Ybt biosynthesis, we measured reporter activity in the YbtA-deficient mutant
211 UTI89Δ*ybtA.* Compared to UTI89, *Yersinia* operon 1 reporter activity in UTI89Δ*ybtA* remained minimal
212 throughout M63+hTf cultures (**Fig. 6e,h**), with a non-significant trend toward lower reporter activity than
213 UTI89Δ*ybtE* at 20 hours (p=0.12)(**Fig. 6f,h)**. Unlike UTI89Δ*ybtE*, the loss of *Yersinia* operon 1 reporter
214 activity in UTI89Δ*ybtA* was not restored by addition of purified Ybt to the culture medium (**Fig. 6g,h**).
215 Although these results do not definitively identify YbtA as a Ybt receptor, they are consistent with this
216 possible role and show that YbtA is necessary for Ybt biosynthetic gene transcription.

217

218 ***Differential Ent and Ybt production is typical of multiple clinical urinary isolates***

219 To determine whether other urinary isolates carrying the *Yersinia* HPI exhibit density-dependent Ybt
220 biosynthetic regulation similar to UTI89, we measured siderophore production by genetically distinctive
221 clinical urinary isolates cultured in M63+hTf (Table 1)[42,43]. In addition to *E. coli*, this included
222 *Citrobacter diversus*, a distinctive *Enterobacterales* species (**Fig. 7f**). We compared siderophore
223 concentrations of Ent and Ybt during early (8 hours) and late (15 hours) time points. As with UTI89, the
224 Ybt:Ent ratio was higher in late than in early time points for all strains examined (**Fig. 7a-f**). These
225 findings are consistent with density-dependent Ybt production in multiple urinary *Enterobacterales*
226 isolates, similar to that observed in UTI89.

227 **DISCUSSION**

228 We find that, during siderophore-dependent growth of UPEC, the Ybt system is not fully
229 functionally redundant with the genetically conserved Ent system. This is attributable to deficient Ybt
230 biosynthesis at low cell density. Full Ybt biosynthesis instead requires a density-dependent transcriptional
231 regulatory cycle in which Ybt acts as an autoinducer (**Fig. 8**). These characteristics are consistent with the
232 quorum-sensing regulation, where cellular crowding leads to extracellular accumulation of an
233 autoinductive signal. While QS control of siderophore system activity has been described in other
234 bacteria[36,44–46], this is the first description of QS signaling and siderophore activity encoded by the same
235 genetic unit, using the same extracellular small molecule effector.

236 A combined siderophore and QS system may possess distinctive advantages. Encoding both
237 functions within a single non-conserved, mobile genetic island is genetically efficient, facilitating
238 horizontal gene transfer. In the canonical model involving a freely diffusible siderophore, this
239 arrangement also limits the metabolic cost of Ybt biosynthesis in conditions where Ybt diffuses away and
240 is unlikely to retrieve or control metal ions in the immediate environment. In higher cell density
241 environments, Ybt sharing among producers and recycling of imported Ybt permits more rapid
242 autoinducer accumulation while minimizing biosynthetic costs[23]. This view of Ybt as a "public good"
243 contrasts with the Ent system, which *E. coli* appear capable of using as a "private good" at low cell
244 density[47] and requires Ent hydrolysis to release imported iron. Density-dependent siderophore activity
245 may be of particular value in iron-limited host niches where bacterial crowding or confinement is typical.
246 These environments may include epithelial surfaces, biofilms, and intracellular compartments. Consistent
247 with this scenario is the previous finding that *ybtS* is the most upregulated UTI89 gene in biofilm-like
248 intracellular bacterial communities (IBCs) residing within bladder epithelial cells during experimental
249 murine UTI[48].

250 QS stimulation may also optimize Ybt interactions with non-iron transition metal ions such as
251 copper. This may be advantageous during bacterial compartmentalization in the phagolysosome where
252 macrophage-like cells intoxicate bacteria with copper, making Ybt chelation especially advantageous.

253 UPEC compartmentalization may thus serve as an environmental cue, engaging the Ybt autoinductive
254 response and maximizing intraphagosomal copper-Ybt (Cu-Ybt) complex formation. In addition to
255 controlling copper disposition, Cu-Ybt catalyzes superoxide dismutation similarly to superoxide
256 dismutases[49]. Cu-Ybt has been recently described to stimulate Ybt biosynthesis[28], possibly through YbtA-
257 dependent Cu-Ybt stimulation, augmented autoinduction, and/or signaling by copper ions released from
258 the complex[23,26]. Whether the Ybt system persists among UPEC due to its iron scavenging activity, its
259 interactions with non-iron metal ions, or both, remains unclear.

260 QS system regulation of siderophore systems has been previously described in other bacterial
261 orders, where the autoinducer and the siderophore are different molecules. In the prototypical quorum-
262 sensing bacterium *Vibrio harveyi*, siderophore production is regulated by the canonical Lux QS system[44]
263 which, unlike the Ybt system, represses siderophore expression with increasing cell density. In
264 *Pseudomonas,* the related LasR QS system increases production of the siderophore pyoverdine with
265 increasing cell density[45]. Both the Lux and Las systems use acylhomoserine lactones as the autoinducer.
266 These varying responses to cellular density may reflect adaptation to different environmental stresses and
267 possibly coordination with different, alternative iron acquisition strategies. Nevertheless, the chemical and
268 regulatory diversity of siderophore systems suggest that bacteria have evolved many strategies to control,
269 acquire, and use transition metal ions in their environments.

270 The *Yersinia* HPI, which is more complex than many siderophore systems, encodes components
271 that are typical of QS system, specifically autoinducer biosynthesis, autoinducer transport, and
272 intracellular receptor/regulator functions[50]. The precise functions of these components and their
273 interactions with non-HPI components are incompletely understood. Previous studies have confirmed that
274 Ybt is internalized by an outer membrane transporter (FyuA)[23,51], suggesting the existence of an
275 intracellular receptor. The most likely candidate for this is YbtA, an AraC-type transcription factor with a
276 well-conserved DNA binding domain, which is encoded as an independent operon (operon 2) in the HPI
277 and controls transcription of multiple HPI operons[40,52,53]. Consistent with the autoregulatory function of a
278 QS system, YbtA is predicted to possess an N-terminal ligand-binding domain typical of AraC family

279 proteins that is a strong candidate Ybt receptor candidate[18,28,40]. We speculate that binding to this domain
280 of Ybt, or a derivative thereof, increases transcription of HPI operons and increases Ybt biosynthesis.
281 Further investigation is necessary to test this hypothesis and to construct a more detailed model for its
282 function in *E. coli* and related *Enterobacterales*, which will help us to better understand the host factors
283 exerting selective pressure on these bacteria.

284 **MATERIALS AND METHODS**

285 **Bacterial strains, and culture conditions.** Bacterial strains, including UTI89 and previously
286 characterized deletion mutants, used in this study are listed in Table 1. For vector transformations, starter
287 cultures were grown on LB agar with antibiotics as appropriate overnight at 37 °C. Ampicillin (100
288 µg/ml; Gold Biotechnology), chloramphenicol (34 µg/ml; Gold Biotechnology), and/or kanamycin (100
289 µg/ml; Gold Biotechnology) we used for selection.

290

291 **Bacterial growth curves.** Bacteria cultures (3 ml LB medium) were grown overnight with continuous
292 shaking at 37 °C. Cells were collected from 1 ml of culture and resuspended in 3 ml of M63 minimal
293 media (0.5 M potassium phosphate, pH 7.4, 10g/liter (NH4)2SO4, 2 mM MgSO4, 0.1 mM CaCl2, 0.2%
294 glycerol, 10 g/ml niacin)[24]. The cells were then grown for 4 hours shaking in 37 °C. 1 ml of cells were
295 collected and washed with fresh M63 media. Before adding the cells to the 96-well round bottom plate,
296 the wells were filled with 200 µl fresh M63 media with or without 3 µM of human transferrin (Sigma-
297 Aldrich #T1147) and incubated at room temperature for 30 minutes. Bacteria were added to the 96-well
298 plate for a starting concentration 0.01 OD (around 8 million CFU). The plate was then grown shaking at
299 37 °C for 20 hours with hourly A_{600} OD measurements using a Tecan SPARK multimode microplate
300 reader with a modular design including an incubator, shaker, and lid lifter (catalog #30086376).

301

302 **Enterobactin extraction.** Enterobactin was isolated using method described in previous
303 publications[10,54]. Fractions containing pure Ent were collected, lyophilized, and resuspended in water.
304 Concentrations of metal-free Ent were determined using the Chrome Azurol S assay[55].

305

306 **Yersiniabactin extraction.** Yersiniabactin was isolated using method describe in pervious
307 publication[28]. Fractions containing pure Ybt were collected, lyophilized, and resuspended in water.
308 Concentrations of metal-free Ybt were determined using the Chrome Azurol S assay[55].

309

310 **Liquid chromatography-mass spectrometry (LC-MS).** LC-MS analyses was conducted with an
311 HPLC–equipped AB Sciex 4000 QTRAP with a Turbo V ESI ion source run in positive ion mode
312 (Shimadzu, Kyoto, Japan). The samples were injected onto a phenylhexyl column (100 by 2.1 mm, 2.7
313 µm particle) (Ascentis Express, Supelco, Bellefonte, PA) with a flow rate of 0.4 ml/min. The following
314 gradient was used: solvent A (0.1% [vol/vol] formic acid) was held constant at 95% and solvent B (90%
315 [vol/vol] acetonitrile, 0.1% [vol/vol] formic acid) at 5% for 2 min. Solvent B was increased to 65% by 6
316 min and to 98% by 8 min. Solvent B was then held constant at 98% until 9 min before it was decreased to
317 5% by 11 min. Solvent B was then held constant at 5% for 1 additional minute. The collision energy was
318 set at 37 V.

319

320 **qRT-PCR of bacterial mRNA.** UTI89 was grown in 500 ml of M63 minimal media with 150 µM
321 2,2'-dipyridyl shaking at 37 °C. RNA was extracted from bacterial cultures using Qiagen RNA isolation
322 kit. RNA was converted to cDNA, using a Thermo Fisher thermocycler, qRT-PCR was run on the cDNA.
323 Primers for *ybtS*, *entB*, along with a housekeeper *rssA,* were used to measure siderophore biosynthesis
324 transcription (**Table S1**).

325

326 **Fluorescent reporter constructs.** Protein expression vector pMAL-c5Xa (NEB) was used as the
327 backbone for constructing the mCherry reporter. The malE gene and the lacI promoter were restricted
328 from the vector using SacI and KasI restriction enzymes. The *entCEBA* promoter was amplified with
329 primers GK073-F/GK073-R (**Table S1**) and inserted into the pMAL-c5Xa backbone. The reporter
330 constructs were transformed into respective strains as indicated. An inducible GFP was made by inserting
331 the *Yersinia* operon 1 promoter sequence into plasmid pFCcGi (Addgene) upon restriction with HindIII
332 and XbaI (NEB). The resulting construct was called *pybtP:GFP*[28]. The reporter constructs were
333 transformed into respective strains as indicated.

334

335 **Flow Cytometry.** The bacterial cells isolated from the bacterial cultures were resuspended in 4%
336 paraformaldehyde PBS to fix the cells. The cells were incubated for 30 minutes at room temperature.
337 After 30 minutes, 1 ml of cold PBS was added to quench the fixative. The cells were resuspended in cold
338 FACS buffer (1% BSA, 0.1% sodium azide in PBS). The cells were then measured on a Cytek Aurora®
339 flow cytometer (N9-20006 Rev. B) using violet, blue, yellow-green, red lasers. SpectroFlo® software and
340 quality control beads were used to control and read the data from the flow cytometer. The data was then
341 analyzed using FlowJo software. Negative FACS gates were determined using non-fluorescent protein
342 contain cultures.

343

344

ACKNOWLEDGEMENTS

J.P.H acknowledges National Institute of Health (NIH) grant R01DK111930 and RO1DK125860. W.H.M. acknowledges NIH funding sources: KL2TR002346, UL1TR002345, 5K08AR076464. We acknowledge Anne Robinson and John Robinson for their insightful discussions. We acknowledge Hung Tran and Anthony Tran for helping make bacterial mutant constructs. We declare no conflicts of interest.

350 **REFERENCES**

351 1. Foxman B. Epidemiology of urinary tract infections: incidence, morbidity, and economic costs.
352 *Am J Med*. 2002;113 Suppl 1A:5S-13S. http://www.ncbi.nlm.nih.gov/pubmed/12113866.
353 Accessed September 9, 2018.

354 2. Ronald A. The etiology of urinary tract infection: traditional and emerging pathogens. *Dis Mon*.
355 2003;49(2):71-82. doi:10.1067/mda.2003.8

356 3. Foxman B, Zhang L, Tallman P, et al. Virulence characteristics of Escherichia coli causing first
357 urinary tract infection predict risk of second infection. *J Infect Dis*. 1995;172(6):1536-1541.
358 http://www.ncbi.nlm.nih.gov/pubmed/7594713. Accessed September 9, 2018.

359 4. Parker KS, Wilson JD, Marschall J, Mucha PJ, Henderson JP. Network Analysis Reveals Sex- and
360 Antibiotic Resistance-Associated Antivirulence Targets in Clinical Uropathogens. *ACS Infect Dis*.
361 2016;1(11):523-532. doi:10.1021/acsinfecdis.5b00022

362 5. Cassat JE, Skaar EP. Iron in Infection and Immunity. *Cell Host Microbe*. 2013;13(5):509.
363 doi:10.1016/J.CHOM.2013.04.010

364 6. Robinson AE, Heffernan JR, Henderson JP. The iron hand of uropathogenic Escherichia coli: The
365 role of transition metal control in virulence. *Future Microbiol*. 2018;13(7):813-829.
366 doi:10.2217/fmb-2017-0295

367 7. Pishchany G, Haley KP, Skaar EP. Staphylococcus aureus growth using human hemoglobin as an
368 iron source. *J Vis Exp*. 2013;(72):1-6. doi:10.3791/50072

369 8. Skaar EP, Humayun M, Bae T, DeBord KL, Schneewind O. Iron-source preference of
370 Staphylococcus aureus infections. *Science (80-)*. 2004;305(5690):1626-1628.
371 doi:10.1126/SCIENCE.1099930/SUPPL_FILE/SKAAR.SOM.PDF

372 9. Aisen P, Leibman A, Zweier J. Stoichiometric and site characteristics of the binding of iron to
373 human transferrin. *J Biol Chem*. 1978;253(6):1930-1937. doi:10.1016/s0021-9258(19)62337-9

374 10. Shields-cutler RR, Crowley JR, Hung CS, et al. Human urinary composition controls antibacterial
375 activity of siderocalin. *J Biol Chem*. 2015;290(26):15949-15960. doi:10.1074/jbc.M115.645812

376 11. Shields-Cutler RR, Crowley JR, Miller CD, Stapleton AE, Cui W, Henderson JP. Human
377 metabolome-derived cofactors are required for the antibacterial activity of siderocalin in urine. *J*
378 *Biol Chem*. 2016;291(50):25901-25910. doi:10.1074/jbc.M116.759183
379 12. Correnti C, Strong RK. Mammalian siderophores, siderophore-binding lipocalins, and the labile
380 iron pool. *J Biol Chem*. 2012;287(17):13524-13531. doi:10.1074/JBC.R111.311829
381 13. Wally J, Buchanan SK. A structural comparison of human serum transferrin and human
382 lactoferrin. In: *BioMetals*. Vol 20. ; 2007:249-262. doi:10.1007/s10534-006-9062-7
383 14. Pan Y, Sonn GA, Sin MLY, et al. Electrochemical immunosensor detection of urinary lactoferrin
384 in clinical samples for urinary tract infection diagnosis. *Biosens Bioelectron*. 2010;26(2):649-654.
385 doi:10.1016/j.bios.2010.07.002
386 15. Chaturvedi KS, Hung CS, Crowley JR, Stapleton AE, Henderson JP. protect pathogens during
387 infection. *Nat Chem Biol*. 2012;8(8):731-736. doi:10.1038/nchembio.1020
388 16. Chen SL, Hung C-S, Xu J, et al. Identification of genes subject to positive selection in
389 uropathogenic strains of Escherichia coli: a comparative genomics approach. *Proc Natl Acad Sci*
390 *U S A*. 2006;103(15):5977-5982. doi:10.1073/pnas.0600938103
391 17. Hunt MD, Pettis GS, Mcintosh MA. *Promoter and Operator Determinants for Fur-Mediated Iron*
392 *Regulation in the Bidirectional FepA-Fes Control Region of the Escherichia Coli Enterobactin*
393 *Gene System*. Vol 176.; 1994. http://jb.asm.org/. Accessed March 28, 2020.
394 18. Fetherston JD, Bearden SW, Perry RD. YbtA, an AraC-type regulator of the Yersinia pestis
395 pesticin/yersiniabactin receptor. *Mol Microbiol*. 1996;22(2):315-325. doi:10.1046/j.1365-
396 2958.1996.00118.x
397 19. Christopher JP, Pistorius E, Axelrod B, et al. *Ferric Uptake Regulation Protein Acts as a*
398 *Repressor, Employing Iron(II) as a Cofactor To Bind the Operator of an Iron Transport Operon in*
399 *Escherichia Colft*. Vol 26.; 1987. https://pubs.acs.org/sharingguidelines.
400 20. Harris WR, Carrano CJ, Cooper SR, et al. Coordination Chemistry of Microbial Iron Transport
401 Compounds . 19 . Stability Constants and Electrochemical Behavior of Ferric Enterobactin and

402 Model Complexes1. *Am Chem Soc*. 1979:6097-6104.

403 21. Koh EI, Henderson JP. Microbial copper-binding siderophores at the host-pathogen interface. *J*
404 *Biol Chem*. 2015;290(31):18967-18974. doi:10.1074/jbc.R115.644328

405 22. Robinson AE, Lowe JE, Koh EI, Henderson JP. Uropathogenic enterobacteria use the
406 yersiniabactin metallophore system to acquire nickel. *J Biol Chem*. 2018;293(39):14953-14961.
407 doi:10.1074/jbc.RA118.004483

408 23. Koh EI, Robinson AE, Bandara N, Rogers BE, Henderson JP. Copper import in Escherichia coli
409 by the yersiniabactin metallophore system. *Nat Chem Biol*. 2017;13(9):1016-1021.
410 doi:10.1038/nchembio.2441

411 24. Henderson JP, Crowley JR, Pinkner JS, et al. Quantitative metabolomics reveals an epigenetic
412 blueprint for iron acquisition in uropathogenic Escherichia coli. *PLoS Pathog*. 2009;5(2).
413 doi:10.1371/journal.ppat.1000305

414 25. Zou Z, Potter RF, McCoy WH, et al. E. coli catheter-associated urinary tract infections are
415 associated with distinctive virulence and biofilm gene determinants. *JCI insight*. 2023;8(2).
416 doi:10.1172/JCI.INSIGHT.161461

417 26. Koh E, Hung CS, Parker KS, Crowley JR, Giblin DE, Henderson JP. Metal selectivity by the
418 virulence-associated yersiniabactin metallophore system Eun-Ik. *Metallomics*. 2015;7(6):1011-
419 1022. doi:10.1039/c4mt00341a.Metal

420 27. Bachman MA, Lenio S, Schmidt L, Oyler JE, Weiser JN. Interaction of Lipocalin 2 , Transferrin ,
421 and Siderophores Determines the Replicative Niche of Klebsiella pneumoniae during Pneumonia.
422 *MBio*. 2012;3(6):1-8. doi:10.1128/mBio.00224-11.Editor

423 28. Katumba GL, Tran H, Henderson JP. The Yersinia High-Pathogenicity Island Encodes a
424 Siderophore-Dependent Copper Response System in Uropathogenic Escherichia coli. *MBio*.
425 2022;13(1). doi:10.1128/MBIO.02391-21

426 29. Troxell B, Hassan HM. Transcriptional regulation by Ferric Uptake Regulator (Fur) in pathogenic
427 bacteria. *Front Cell Infect Microbiol*. 2013;3(OCT). doi:10.3389/FCIMB.2013.00059

428 30. Teixidó L, Carrasco B, Alonso JC, Barbé J, Campoy S. Fur Activates the Expression of
429 Salmonella enterica Pathogenicity Island 1 by Directly Interacting with the hilD Operator In Vivo
430 and In Vitro. *PLoS One*. 2011;6(5):19711. doi:10.1371/JOURNAL.PONE.0019711
431 31. Delany I, Rappuoli R, Scarlato V. Fur functions as an activator and as a repressor of putative
432 virulence genes in Neisseria meningitidis. *Mol Microbiol*. 2004;52(4):1081-1090.
433 doi:10.1111/J.1365-2958.2004.04030.X
434 32. García-Lara J, Shang LH, Rothfield LI. An extracellular factor regulates expression of sdiA, a
435 transcriptional activator of cell division genes in Escherichia coli. *J Bacteriol*. 1996;178(10):2742-
436 2748. doi:10.1128/JB.178.10.2742-2748.1996
437 33. Sperandio V, Torres AG, Girón JA, Kaper JB. Quorum sensing is a global regulatory mechanism
438 in enterohemorrhagic Escherichia coli O157:H7. *J Bacteriol*. 2001;183(17):5187-5197.
439 doi:10.1128/JB.183.17.5187-5197.2001
440 34. Yang S, Lopez CR, Zechiedrich EL. Quorum sensing and multidrug transporters in Escherichia
441 coli. *Proc Natl Acad Sci U S A*. 2006;103(7):2386-2391.
442 doi:10.1073/PNAS.0502890102/SUPPL_FILE/02890FIG6.PDF
443 35. Wang L, Li J, March JC, Valdes JJ, Bentley WE. luxS-dependent gene regulation in Escherichia
444 coli K-12 revealed by genomic expression profiling. *J Bacteriol*. 2005;187(24):8350-8360.
445 doi:10.1128/JB.187.24.8350-8360.2005/ASSET/03550AA2-7A4D-49CA-BCF1-
446 A426E540423F/ASSETS/GRAPHIC/ZJB0240553010007.JPEG
447 36. McRose DL, Baars O, Seyedsayamdost MR, Morel FMM. Quorum sensing and iron regulate a
448 two-for-one siderophore gene cluster in Vibrio harveyi. *Proc Natl Acad Sci U S A*.
449 2018;115(29):7581-7586. doi:10.1073/pnas.1805791115
450 37. Lewenza S, Sokol PA. Regulation of ornibactin biosynthesis and N-acyl-L-homoserine lactone
451 production by cepR in Burkholderia cepacia. *J Bacteriol*. 2001;183(7):2212-2218.
452 doi:10.1128/JB.183.7.2212-2218.2001/ASSET/12A0813A-D644-4575-8FEE-
453 D848E1708B51/ASSETS/GRAPHIC/JB0711270003.JPEG

454 38. Lewenza S, Conway B, Greenberg EP, Sokol PA. Quorum sensing in Burkholderia cepacia:
455 identification of the LuxRI homologs CepRI. *J Bacteriol*. 1999;181(3):748-756.
456 doi:10.1128/JB.181.3.748-756.1999
457 39. Wen Y, Kim IH, Son JS, Lee BH, Kim KS. Iron and Quorum Sensing Coordinately Regulate the
458 Expression of Vulnibactin Biosynthesis in Vibrio vulnificus. *J Biol Chem*. 2012;287(32):26727.
459 doi:10.1074/JBC.M112.374165
460 40. Anisimov R, Brem D, Heesemann J, Rakin A. Transcriptional regulation of high pathogenicity
461 island iron uptake genes by YbtA. *Int J Med Microbiol*. 2005;295(1):19-28.
462 doi:10.1016/J.IJMM.2004.11.007
463 41. Fetherston JD, Bearden SW, Perry RD. YbtA, an AraC-type regulator of the Yersinia pestis
464 pesticin/yersiniabactin receptor. *Mol Microbiol*. 1996;22(2):315-325. doi:10.1046/J.1365-
465 2958.1996.00118.X
466 42. Hultgren SJ, Schwan WR, Schaeffer AJ, Duncan JL. Regulation of production of type 1 pili
467 among urinary tract isolates of Escherichia coli. *Infect Immun*. 1986;54(3):613-620.
468 doi:10.1128/IAI.54.3.613-620.1986
469 43. Ohlemacher SI, Giblin DE, D'Avignon DA, Stapleton AE, Trautner BW, Henderson JP.
470 Enterobacteria secrete an inhibitor of Pseudomonas virulence during clinical bacteriuria. *J Clin*
471 *Invest*. 2017;127(11):4018-4030. doi:10.1172/JCI92464
472 44. Eickhoff MJ, Fei C, Cong JP, Bassler BL. LuxT Is a Global Regulator of Low-Cell-Density
473 Behaviors, Including Type III Secretion, Siderophore Production, and Aerolysin Production, in
474 Vibrio harveyi. *MBio*. 2022;13(1). doi:10.1128/MBIO.03621-21/SUPPL_FILE/MBIO.03621-21-
475 ST001.DOCX
476 45. Stintzi A, Evans K, Meyer JM, Poole K. Quorum-sensing and siderophore biosynthesis in
477 Pseudomonas aeruginosa: lasR/lasI mutants exhibit reduced pyoverdine biosynthesis. *FEMS*
478 *Microbiol Lett*. 1998;166(2):341-345. doi:10.1111/J.1574-6968.1998.TB13910.X
479 46. Lewenza S, Sokol PA. Regulation of ornibactin biosynthesis and N-acyl-L-homoserine lactone

480 production by CepR in Burkholderia cepacia. *J Bacteriol*. 2001;183(7):2212-2218.
481 doi:10.1128/JB.183.7.2212-2218.2001
482 47. Scholz RL, Greenberg EP. Sociality in Escherichia coli: Enterochelin is a private good at low cell
483 density and can be shared at high cell density. *J Bacteriol*. 2015;197(13):2122-2128.
484 doi:10.1128/JB.02596-14
485 48. Mysorekar IU, Hultgren SJ. Mechanisms of uropathogenic Escherichia coli persistence and
486 eradication from the urinary tract. *Proc Natl Acad Sci U S A*. 2006;103(38):14170-14175.
487 doi:10.1073/PNAS.0602136103/SUPPL_FILE/02136FIG10.PDF
488 49. Chaturvedi KS, Hung CS, Giblin DE, et al. Cupric yersiniabactin is a virulence-associated
489 superoxide dismutase mimic. *ACS Chem Biol*. 2014;9(2):551-561. doi:10.1021/cb400658k
490 50. Schubert S, Rakin A, Heesemann J. The Yersinia high-pathogenicity island (HPI): evolutionary
491 and functional aspects. *Int J Med Microbiol*. 2004;294(2-3):83-94.
492 doi:10.1016/J.IJMM.2004.06.026
493 51. Lukacik P, Barnard TJ, Keller PW, et al. Structural engineering of a phage lysin that targets Gram-
494 negative pathogens. *Proc Natl Acad Sci U S A*. 2012;109(25):9857-9862.
495 doi:10.1073/PNAS.1203472109/-/DCSUPPLEMENTAL
496 52. Gao H, Zhou D, Li Y, et al. The iron-responsive fur regulon in Yersinia pestis. *J Bacteriol*.
497 2008;190(8):3063-3075. doi:10.1128/JB.01910-07
498 53. Perry RD, Fetherston JD. Yersinia pestis--etiologic agent of plague. *Clin Microbiol Rev*.
499 1997;10(1):35. doi:10.1128/CMR.10.1.35
500 54. Guo C, Steinberg LK, Cheng M, Song JH, Henderson JP, Gross ML. Site-Specific Siderocalin
501 Binding to Ferric and Ferric-Free Enterobactin As Revealed by Mass Spectrometry. *ACS Chem*
502 *Biol*. 2020;15(5):1154-1160. doi:10.1021/ACSCHEMBIO.9B00741
503 55. Schwyn B, Neilands JB. Universal chemical assay for the detection and determination of
504 siderophores. *Anal Biochem*. 1987;160(1):47-56. doi:10.1016/0003-2697(87)90612-9
505 56. Chen SL, Hung C-S, Xu J, et al. Identification of genes subject to positive selection in

506 uropathogenic strains of Escherichia coli: a comparative genomics approach. *Proc Natl Acad Sci*
507 *U S A*. 2006;103(15):5977-5982. doi:10.1073/pnas.0600938103
508 57. Lv H, Henderson JP. Yersinia high pathogenicity Island genes modify the Escherichia coli primary
509 metabolome independently of siderophore production. *J Proteome Res*. 2011;10(12):5547-5554.
510 doi:10.1021/pr200756n
511
512
513
514
515
516
517
518
519
520
521
522
523
524
525
526
527
528
529
530
531
532
533

534 **Table 1: Bacterial strains used in this study**

535

Strain	Phenotype	Ref.
UTI89	clinical isolate of acute cystitis	56
UTI89Δ*ybtS*	Ybt-deficient UTI89 deletion mutant	57
UTI89Δ*ybtSΔiroB*	Ybt-deficient and salmochelin-deficient UTI89 deletion mutant	24
UTI89Δ*entB*	Ent-deficient and salmochelin-deficient UTI89 deletion mutant	24
UTI89Δ*entBΔybtS*	Ent-deficient, Ybt-deficient and salmochelin-deficient (siderophore-null) UTI89 deletion mutant	57
UTI89Δ*ybtE*	Ybt-deficient UTI89 deletion mutant	57
UTI89Δ*fur*	Fur deletion mutant lacking iron-mediated Fur repression	57
UTI89Δ*ybtA*	*ybtA* deletion mutant lacking HPI encoded transcription activator	57
UTI89 *p:entC-mCherry_p:ybtP-GFP*	UTI89 with GFP-*ybtP* and mCherry-*entC* reporter plasmids	*this work*
UTI89*ΔybtE_ p:entC-mCherry_p:ybtP-GFP*	Ybt-deficient UTI89 deletion mutant with GFP-*ybtP* and mCherry-*entC* reporter plasmids	*this work*
UTI89*ΔentB_ p:entC-mCherry_p:ybtP-GFP*	Ent-deficient and salmochelin-deficient UTI89 deletion mutant with GFP-*ybtP* and mCherry-*entC* reporter plasmids	*this work*
UTI89*ΔentBΔybtS_p:entC-mCherry_p:ybtP-GFP*	Ent-deficient, Ybt-deficient and salmochelin-deficient (siderophore-null) UTI89 deletion mutant with GFP-*ybtP* and mCherry-*entC* reporter plasmids	*this work*
UTI89*Δfur_p:entC-mCherry_p:ybtP-GFP*	Fur deletion mutant lacking iron-mediated Fur repression with GFP-*ybtP* and mCherry-*entC* reporter plasmids	*this work*
UTI89*ΔybtA_p:entC-mCherry_p:ybtP-GFP*	*ybtA* deletion mutant lacking HPI encoded transcription activator with GFP-*ybtP* and mCherry-*entC* reporter plasmids	*this work*
JPH518	*E. coli* ST131 strain isolated from a UTI patient	25
JPH530	*E. coli* ST131 strain isolated from a UTI patient	25
JPH544	*E. coli* ST131 strain isolated from a UTI patient	25
JPH557	*E. coli* ST131 strain isolated from a UTI patient	25
NU-14	UTI model strain	43
SJH734 (*C. diversus*)	*Citrobacter* strain isolated from a UTI patient	43

536
537
538
539
540
541
542
543
544
545
546
547
548
549

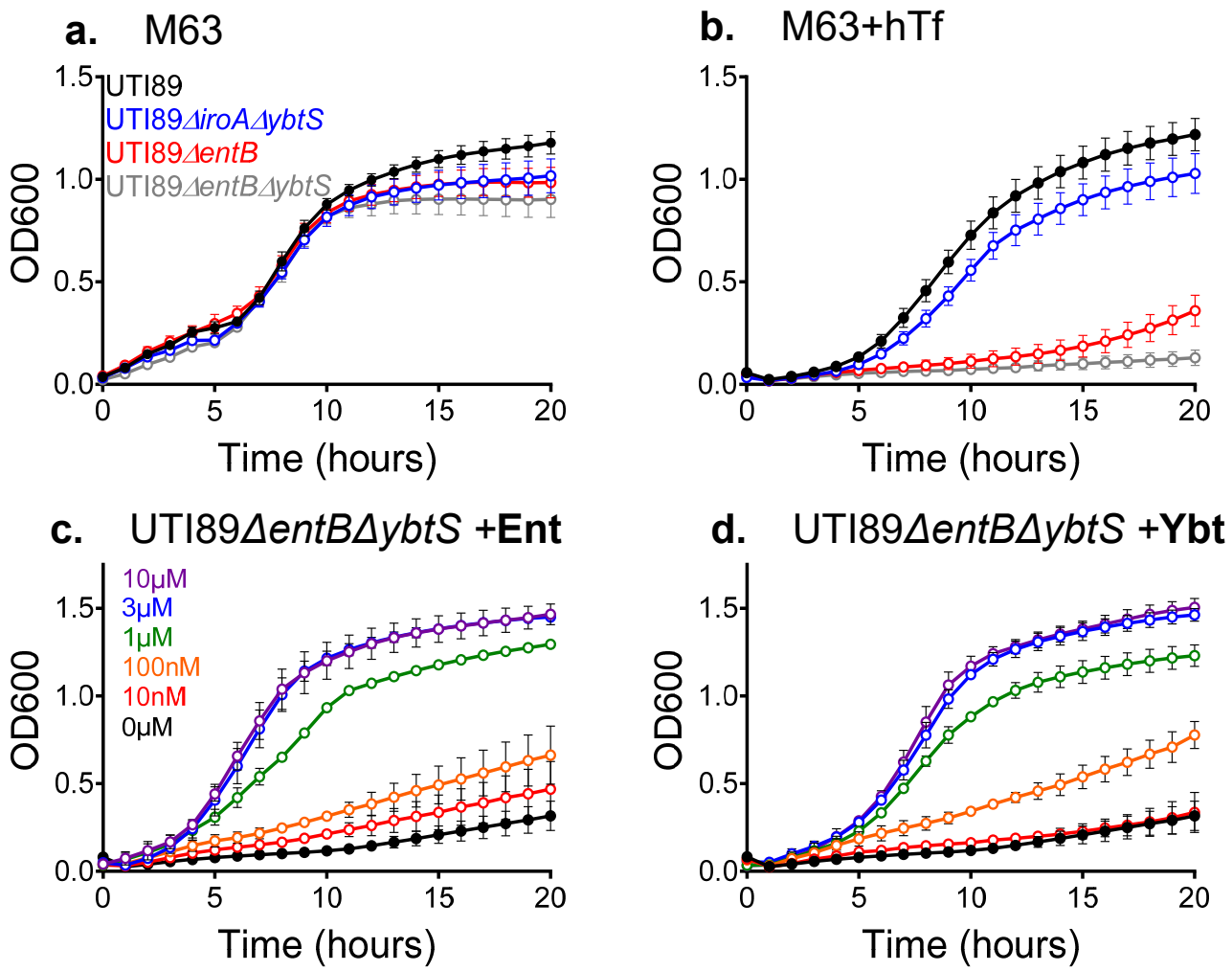

Figure 1. Yersiniabactin (Ybt) biosynthesis does not compensate for loss of enterobactin (Ent) biosynthesis during siderophore-dependent growth of *E. coli* UTI89 and isogenic mutants. (a,b) Growth curves of UTI89 and isogenic siderophore biosynthesis mutants in M63/glycerol media in the absence (a) or presence of 3 μM human *apo*-transferrin (hTf, b). (c,d). Growth curves of the complete siderophore biosynthesis-deficient mutant UTI89*ΔentBΔybtS* in M63+hTf containing increasing concentrations of purified Ent (c), or Ybt(d).

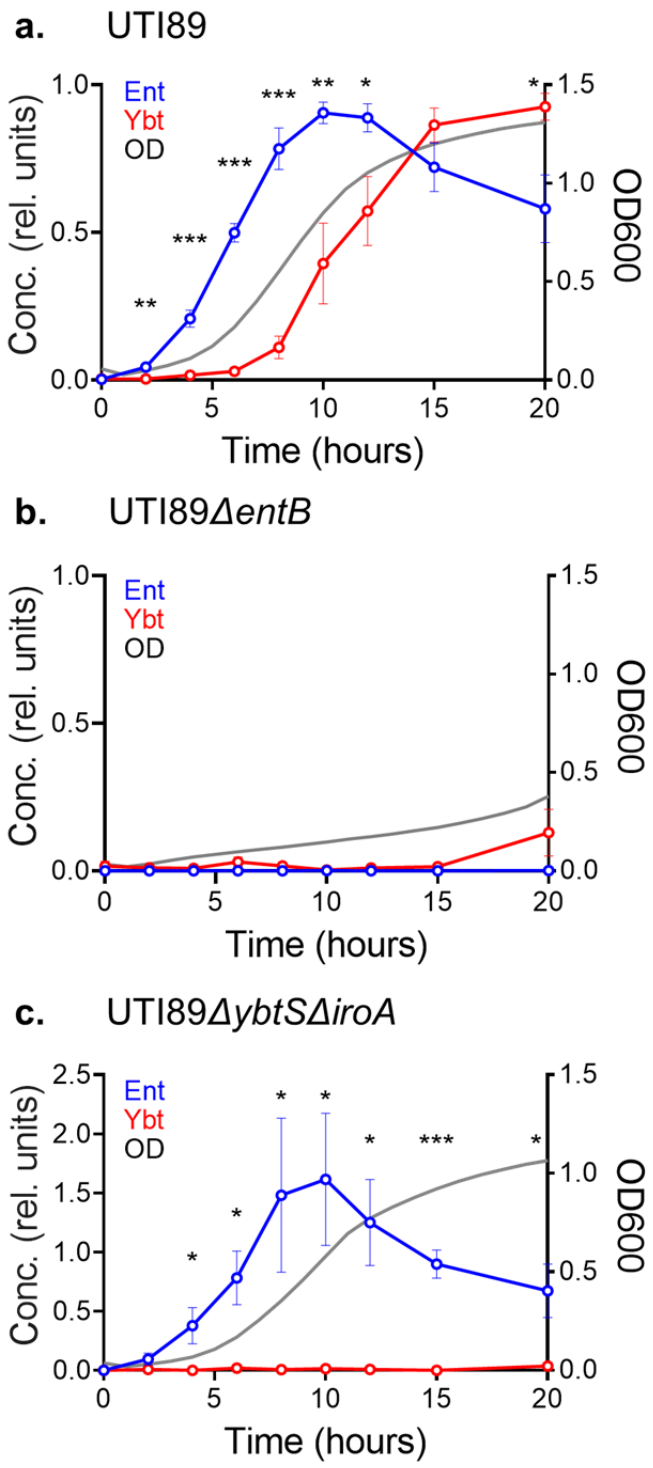

Figure 2. Time course of Ent and Ybt production by *E. coli* UTI89 and isogenic mutants. Liquid chromatography-mass spectrometry was used to quantify Ent (blue) and Ybt (red) content of M63+hTf medium conditioned by wild type UTI89 (a), UTI89*ΔentB*(b), or UTI89*ΔybtSΔiroA*(c) over 20 hours. Concentration values are relative to maximum values in UTI89. Culture density (optical density at 600 nm) is depicted by the gray plot line. Statistical comparison between relative conc. of Ent and Ybt at each time point: *, $P < 0.05$; **, $P < 0.01$; ***, $P < 0.001$ by unpaired T-test.

561

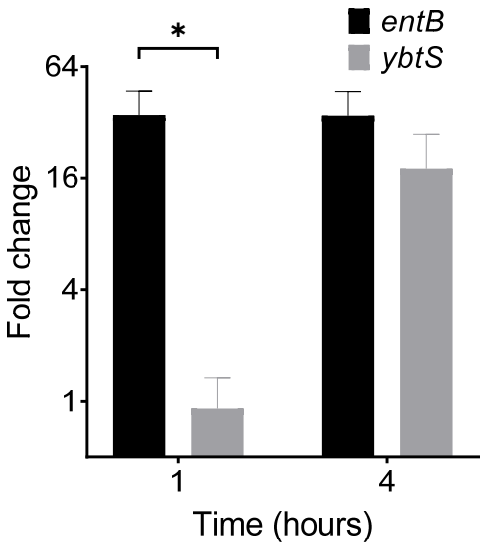

562

563

564 **Figure 3. Early siderophore biosynthetic gene transcription in UTI89 assessed by qRT-**
565 **PCR during siderophore-dependent growth.** mRNA fold change of *entB* and *ybtS* biosynthesis
566 gene expression at 1 and 4 hours in M63 media containing 150 µM 2,2'-dipyridyl, normalized to
567 10 hour time point. *rssA* was used as a housekeeper gene. *, $P < 0.05$ using unpaired T-test.

568

569

570

571

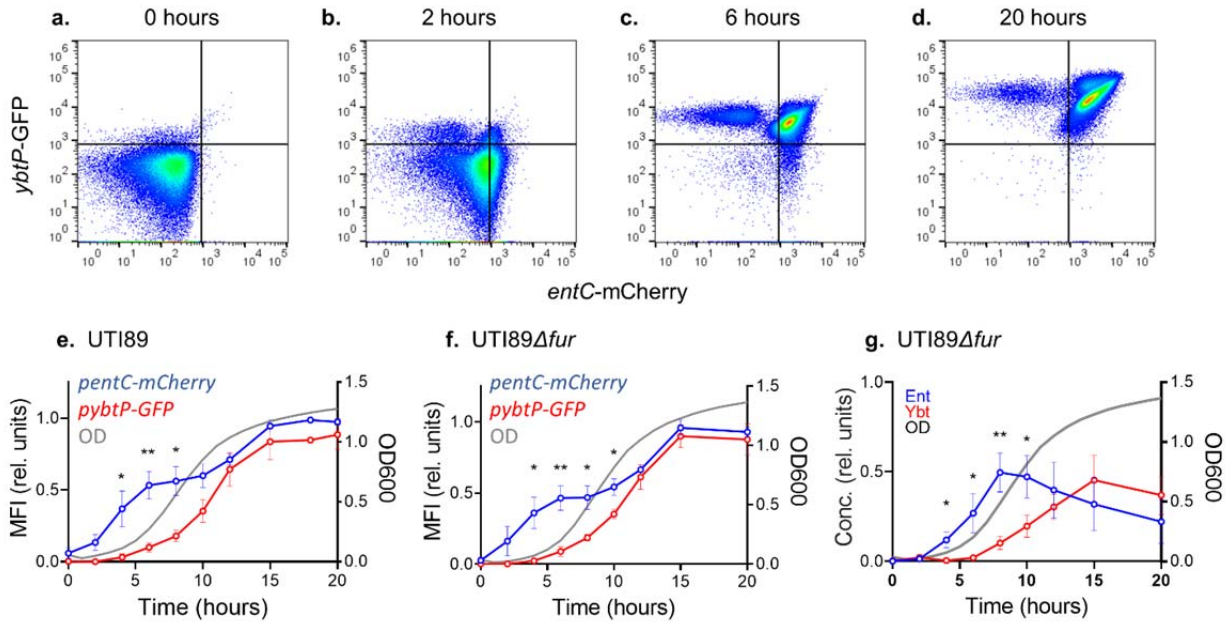

572

573

574 **Figure 4. Siderophore biosynthetic operon transcription in UTI89 and its *fur*-deficient**
575 **mutant assessed by fluorescent reporter expression during siderophore-dependent growth.**
576 Fluorescent protein expression in bacterial cultures was measured using flow cytometry. GFP
577 fluorescence controlled by the *Yersinia* operon 1 promoter (*ybtP*-GFP) and mCherry
578 fluorescence controlled by the *entCEBA* promoter (*entC*-mCherry) are displayed. (a-d)
579 Representative pseudocolor plots of UTI89 *p:entC-mCherry p:ybtP-GFP* at 0, 2, 6, and 20 hours.
580 Quadrants are gated on non-fluorescent protein cultures. (e,f) Mean fluorescence intensity (MFI)
581 for each reporter of normalized to WT during growth of UTI89 *p:entC-mCherry p:ybtP-GFP* (e)
582 or UTI89*Δfur p:entC-mCherry p:ybtP-GFP* (f) in M63+hTF. (g) Ent and Ybt concentrations
583 relative to wild type (UTI89) in M63+hTf medium conditioned by UTI89*Δfur*. Culture density
584 (optical density at 600 nm) is depicted by the gray plot line. Statistical comparison between
585 relative MFI of *p:entC-mCherry* and *p:ybtP-GFP* at each time point: *, $P < 0.05$; **, $P < 0.01$;
586 ***, $P < 0.001$ by unpaired T-test.

587

588

589

590

591

592

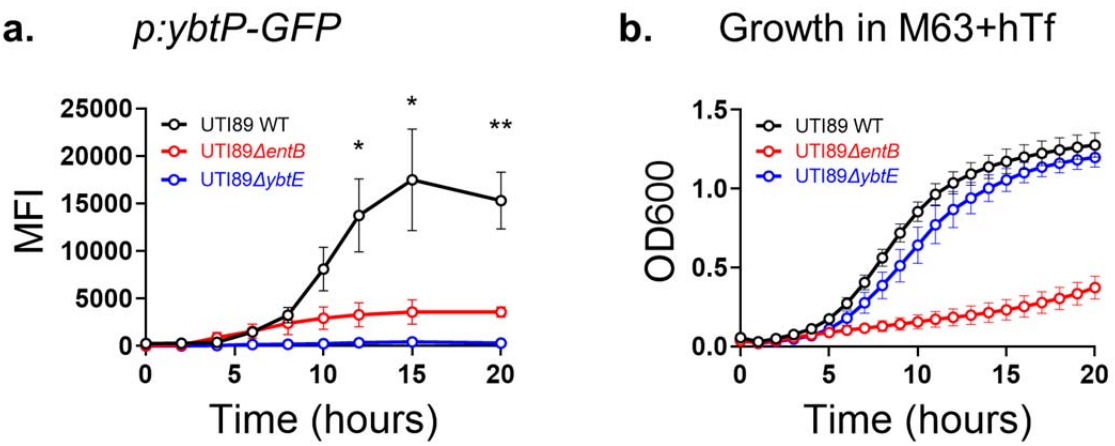

593

594

595 **Figure 5. Lack of growth or loss of Ybt biosynthesis represses *Yersinia* operon 1 expression.**
596 UTI89 strains carrying the *p:entC-mCherry* and *p:ybtP-GFP* plasmids were grown in M63+hTf.
597 *p:ybtP-GFP* reporter expression is displayed as mean fluorescence intensity (MFI) of flow
598 cytometry measurements (a) and growth measured by optical density (OD600, b). Statistical
599 comparison between WT and both mutant strains of the MFI of *p:ybtP-GFP* at each time point:
600 *, $P < 0.05$; **, $P < 0.01$; ***, $P < 0.001$ by unpaired T-test.
601

602

603

604

605

606

607

608

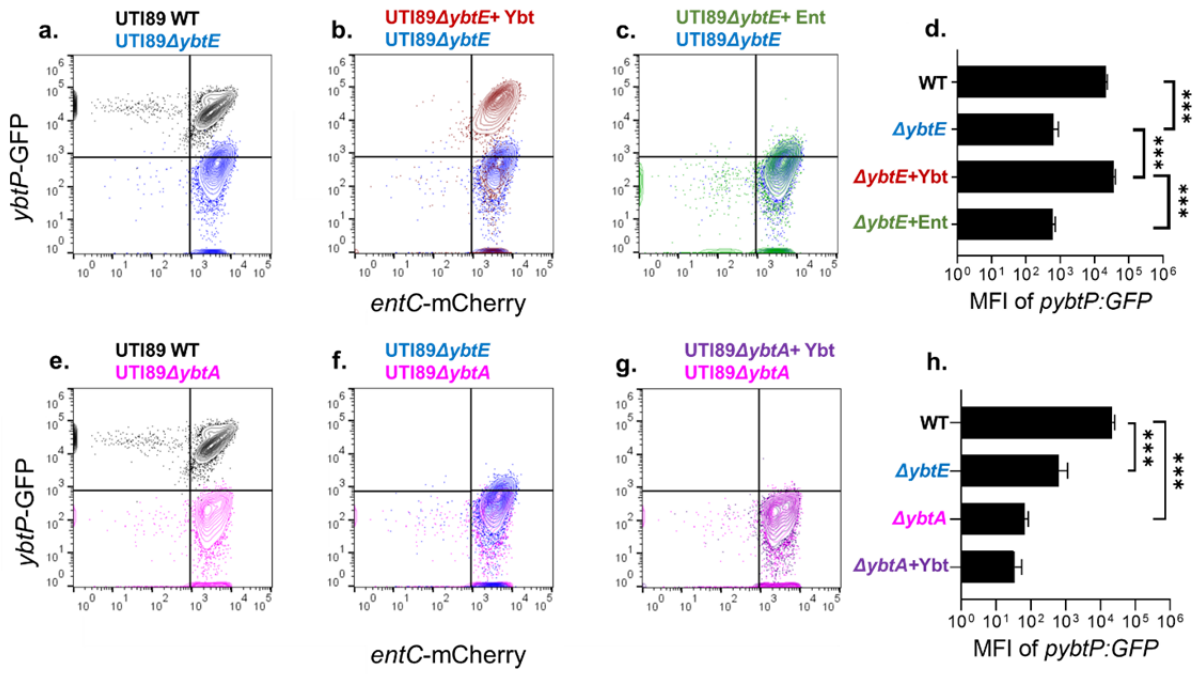

Figure 6. Siderophore biosynthetic operon transcription in UTI89, UTI89 mutants, and with chemically complemented cultures assessed by fluorescent reporter expression. (a-c, e-g) Representative pseudocolor plots of strains transfected with *p:entC-mCherry* and *p:ybtP-GFP* after 20 hours of growth in M63+hTf. Quadrants are gated on non-fluorescent protein cultures. (d,h) Mean fluorescence intensity (MFI) of *ybtP*-mCherry from each strain at 20 hours. Culture medium was supplemented with 10 nM Ybt (+Ybt, b,d,g,h) or Ent (+Ent, c,d). *, $P < 0.05$; **, $P < 0.01$; ***, $P < 0.001$ by unpaired T-test.

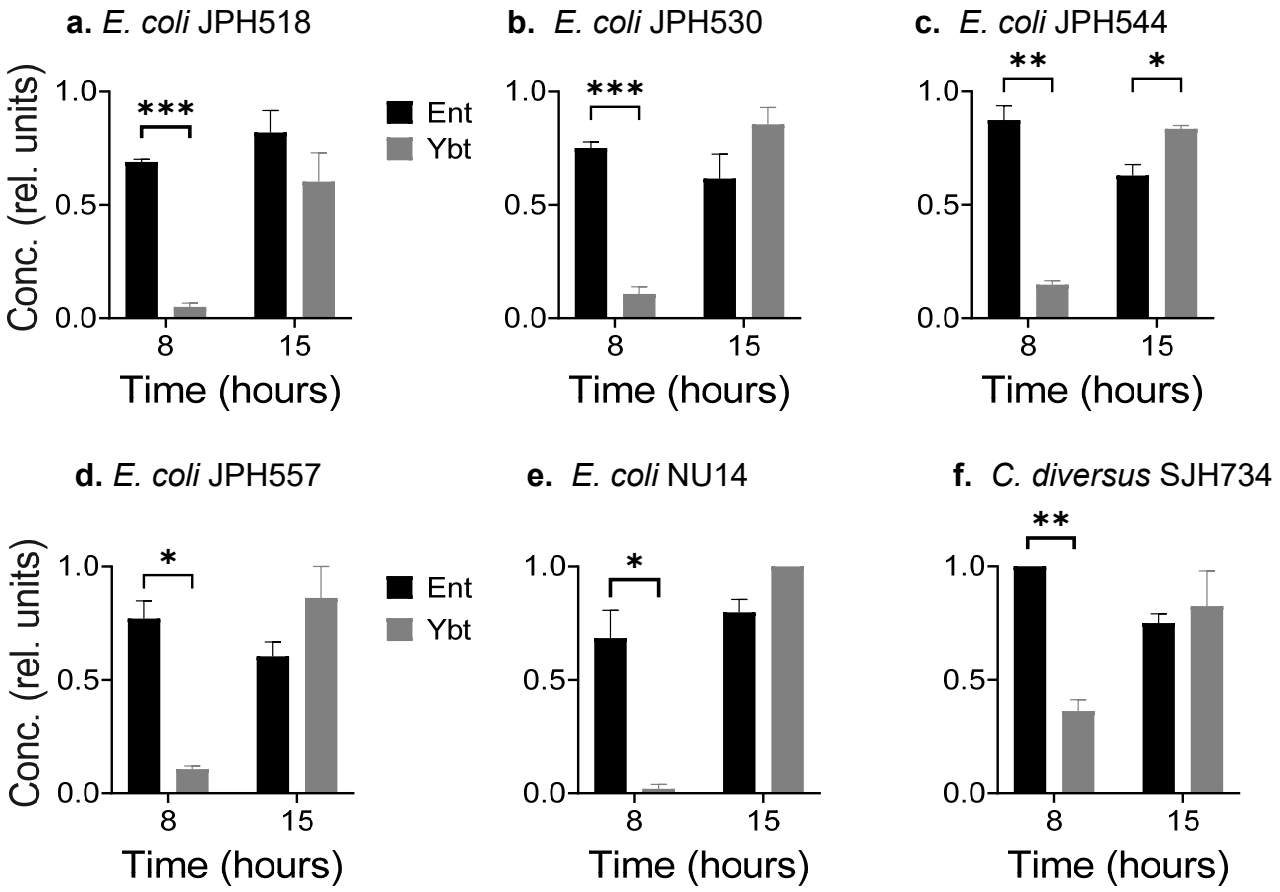

Figure 7. Siderophore production by clinical urinary isolates. Ent and Ybt concentrations relative to UTI89 in M63+hTf medium. Results at early (8 hour) and late (15 hour) time points are displayed for different *E.coli* (a-e) and *Citrobacter diversus,* f). *, $P < 0.05$; **, $P < 0.01$; ***, $P < 0.001$ by unpaired T-test.

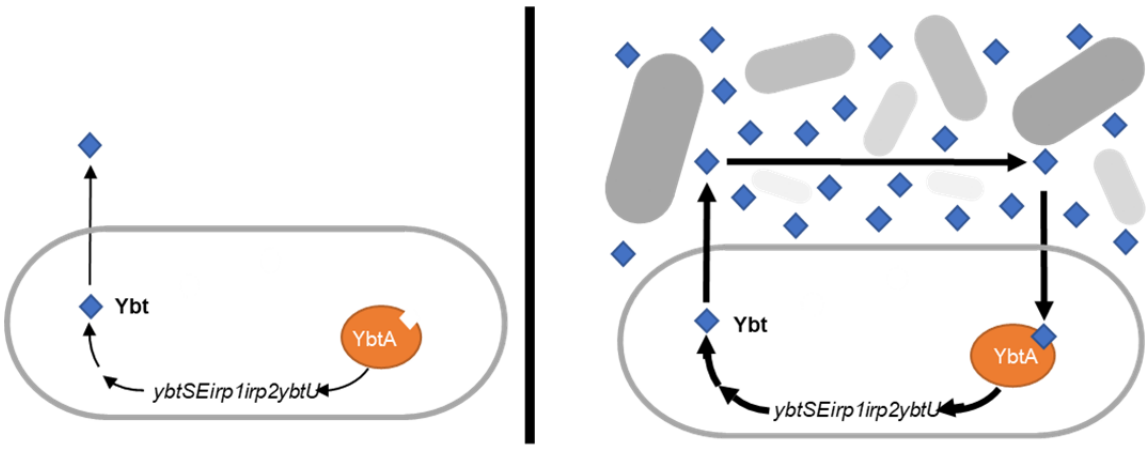

Figure 8: Model of Ybt-mediated quorum sensing autoregulation. At low cell density and limited iron availability (*left*), Ybt biosynthesis is insufficient to match the iron uptake activity of the Ent system. Extracellular Ybt accumulates slowly and autoinduction is minimal. With increasing cell density (*right*), extracellular Ybt accumulates sufficiently to bind YbtA and stimulate increased Ybt biosynthesis by each cell. This autoinductive cycle rapidly increases extracellular Ybt as cell density increases.